

Using Lifetime and Quenching Rate Constant to Determine Optimal Quencher Concentration

Xena L. Soto and John R. Swierk*

Cite This: *ACS Omega* 2022, 7, 25532–25536

Read Online

ACCESS |



Metrics & More

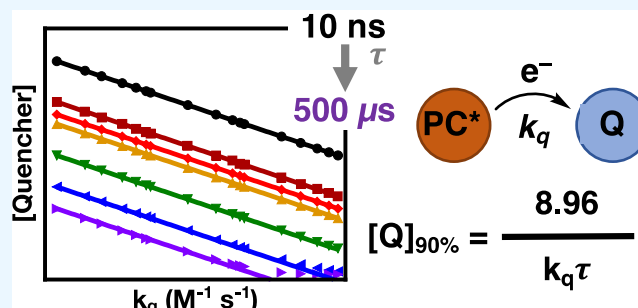


Article Recommendations



Supporting Information

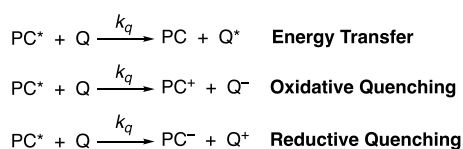
ABSTRACT: Excited state quenching is a key step in photochemical reactions that involve energy or electron transfer. High reaction quantum yields require sufficiently high concentrations of a quencher to ensure efficient quenching. The determination of quencher concentrations is typically done through trial and error. Using kinetic modeling, however, a simple relationship was developed that predicts the concentration of quencher necessary to quench 90% of excited states, using only the photosensitizer lifetime and the rate constant for quenching as inputs. Comparison of the predicted quencher concentrations and quencher concentrations used in photoredox reactions featuring acridinium-based photocatalysts reveals that the majority of reactions used quencher concentrations significantly below the predicted concentration. This suggests that these reactions exhibit low quantum yields, requiring long reaction times and/or intense light sources.



INTRODUCTION

Quenching an excited state is a key step in photochemical reactions that involve electron or energy transfer (Scheme 1).¹

Scheme 1. Quenching Pathways for Excited Photosensitizers (PS*)



Poor kinetics at the quenching step lead to inefficient harvesting of excited states and limit the overall quantum yield of the reaction. As a second-order process, the rate of quenching depends on the concentration of excited photosensitizers, the concentration of the quencher (Q), and the rate constant for quenching (k_q). The quenching step, however, is in direct competition with the unproductive relaxation of the excited state, which is controlled by the lifetime of the photosensitizer (τ). From a reaction design standpoint, the choice of the photosensitizer controls τ , though other factors such as redox potentials and absorption range often take higher priority in the selection of the photosensitizer.² The value of k_q depends on a host of factors including the choice of the substrate, driving force for electron/energy transfer, and degree of association in solution.^{3–5} While k_q can also be tuned in a number of ways (e.g., changing the photosensitizer or substrate, changing the solvent, and adding inert salts), these

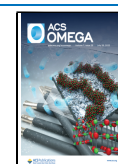
can be impractical from a reaction design standpoint where specific reaction conditions are needed to produce a given product, simplify purification, or solubilize one or more reagents. In principle, the concentration of excited photosensitizers can be varied with light intensity, though as shown below, that has little impact on the quenching yield. Thus, the most practical parameter that can be varied to impact quenching rates and efficiency is the concentration of the quencher. However, instead of quantitatively predicting ideal quencher conditions, trial and error is typically used to determine the optimal concentration in the design of new photochemical reactions.

We hypothesized that, using only k_q and τ , the Stern–Volmer equation could be used to make simple predictions about the quencher concentration needed for efficient excited state quenching. Photosensitizer lifetimes are widely reported for both organic and inorganic photosensitizers.^{1,5,6} Determination of k_q for a photochemical reaction is simple using the Stern–Volmer relationship and is commonly reported. In the simplest formulation of Stern–Volmer, all that is needed is a fluorimeter, an emissive photosensitizer, and knowledge of τ to determine a value for k_q . Inspired by our recent success using

Received: April 28, 2022

Accepted: June 28, 2022

Published: July 12, 2022



kinetic modeling to reproduce reaction quantum yields, we set out to test the hypothesis that with knowledge of k_q and τ , the Stern–Volmer equation could be used as a simple, predictive model to determine the quencher concentration needed to ensure high quenching yields.^{7,8}

RESULTS AND DISCUSSION

Using Kinetiscope,⁹ a freeware stochastic kinetic simulator widely used to study chemical reactions,^{10–12} we developed a simple model that involved competition between the relaxation of the excited state and quenching by a quencher, Q. Our specific reaction involved an oxidative quenching reaction that generated a reduced quencher, $Q^{\bullet-}$, and an oxidized photosensitizer; however, the result would be unchanged for a reductive quenching or energy transfer. Relaxation, k_{relax} , is a first-order process controlled by τ ($k_{\text{relax}} = 1/\tau$), while k_q was varied from $10^7 \text{ M}^{-1} \text{ s}^{-1}$ to $10^{10} \text{ M}^{-1} \text{ s}^{-1}$. Values of k_q greater than $10^{10} \text{ M}^{-1} \text{ s}^{-1}$ were not explored, as these indicate a reaction that is not diffusion-controlled and requires pre-association of a photosensitizer and a quencher or an intramolecular energy/electron transfer. Initially, we modeled continuous illumination and varied the concentration of Q to achieve a quantum yield for quenching, Φ_{quench} , of 0.900 ± 0.001 at the end of the simulation. In this case, Φ_{quench} is defined as the final concentration of $[Q^{\bullet-}]$ divided by the number of photons introduced to the reaction. Targeting a value of 0.900 ± 0.001 for Φ_{quench} represented an optimal balance of harvesting a high concentration of excited states at quencher concentrations that could be practical. We did not regenerate the oxidized photosensitizer in our reaction; however, the concentration of the photosensitizer was relatively high ($100 \mu\text{M}$), the length of the simulation was kept short (1 s), and the illumination intensity was kept to 1.63×10^{-5} photons/s, which corresponds to a 10 mW intensity of 415 nm light. As a result, only a relatively small concentration of photosensitizer was oxidized during the simulation. In addition, increasing both the simulation time and illumination intensity (Figures S2 and S3) resulted in no change in Φ_{quench} , indicating that the buildup of the oxidized photosensitizer has negligible impact on the reaction.

As shown in Figure 1A, varying k_q for a given value of τ resulted in 2–3 orders of magnitude variation in the predicted concentration of the quencher. To our delight, for a given photosensitizer lifetime, the predicted values of [Q] could be fit to a simple power law equation of the form

$$[Q] = \alpha/k_q \quad (1)$$

At short values of τ , the fit to eq 1 was excellent with an R^2 value of 1. At longer values of τ (e.g., $500 \mu\text{s}$), the fit was less accurate at larger k_q values ($>10^9 \text{ M}^{-1} \text{ s}^{-1}$). This is because at those values, the concentration of quencher needed was essentially independent of k_q due to the extremely large values of τ . Figure 1B shows a plot of the value of α as a function of τ and demonstrates that data could also be described by a power law equation of the form

$$\alpha = A/\tau \quad (2)$$

From the fit in Figure 1B, a value of 8.96 was determined for A. Thus, combining eqs 1 and 2, as well as the value for A, the concentration of Q needed to give Φ_{quench} of 0.9 at a given value of τ and k_q is given by eq 3

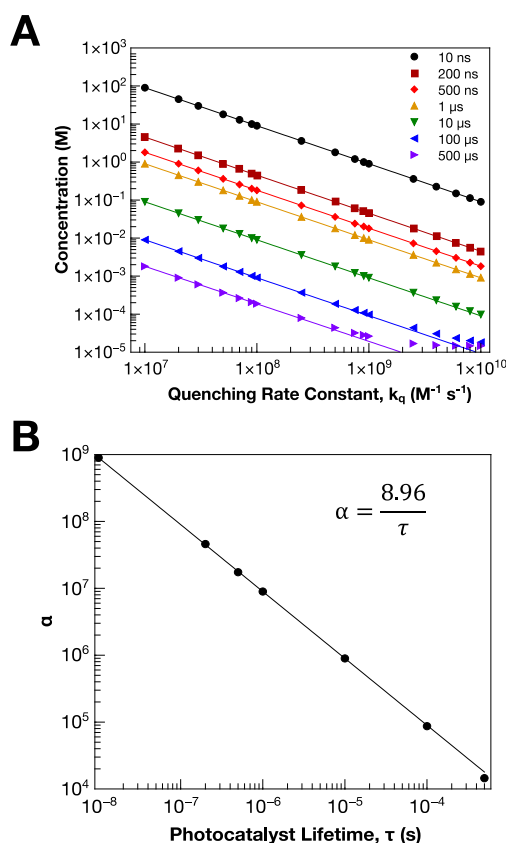


Figure 1. (A) Predicted concentration of the quencher needed to achieve quenching of 90% of excited states as a function of quenching rate constant (k_q) and photosensitizer lifetime. Modeled with continuous illumination of 1.63×10^{-5} photons/s. Solid lines are fit to power law equation of the general form k_q/α . (B) Value of α as a function of photosensitizer lifetime (τ). Solid black line is fit to the equation: $\alpha = 8.96\tau$.

$$[Q] = \frac{8.96}{k_q \tau} \quad (3)$$

For values of τ less than or equal to $10 \mu\text{s}$, the deviation between [Q] predicted from kinetic modeling and [Q] predicted by eq 3 was 5% or less and typically 1–2% at most. For longer values of τ , the values predicted by eq 3 showed significant deviation at values of k_q less than $10^9 \text{ M}^{-1} \text{ s}^{-1}$ and much smaller deviations at smaller values of k_q . Percent deviations are shown in Table S1. We note that the majority of photosensitizers used in photochemical reactions have τ on the order of $10 \mu\text{s}$ or shorter, and in the cases of longer τ values, the kinetic modeling overestimates the concentration of Q needed because of the small quencher concentrations need to achieve 90% quenching. As expected, eq 3 closely matches a rearranged version of the Stern–Volmer equation. If I_0/I is set to 10 to account for 90% of excited states being quenched, then the Stern–Volmer equation rearranges to

$$[Q] = \frac{9}{k_q \tau} \quad (4)$$

This confirms both the validity of using kinetic modeling to study the quenching steps in photochemical reactions and the Stern–Volmer relationship that can be used to predict quencher concentrations needed for efficient harvesting of excited states.

We also performed a similar analysis as above but started with a fixed concentration of excited photosensitizer. This simulates pulsed illumination, like in a laser experiment, where a brief, intense pulse of light excites a significant number of photosensitizers, followed by a dark period. As our benchmark, we set a value of Φ_{quench} of 0.9 after 100 ns of reaction time. Again, this represented a balance between a high value of Φ_{quench} and reasonable concentrations of Q . We also limited our investigation to photosensitizers with lifetimes of 200 ns to 10 μ s. As with continuous illumination, the data could be well fit to eq 1 (Figure S3); however, the plot of α versus τ did not follow the form of eq 2 (Figure S4). As τ gets longer, Figure S3 shows that Φ_{quench} has less of a concentration dependence, likely because relaxation becomes a minor unproductive pathway on the timescale of 100 ns.

In order to further validate the results from our simulations, we calculated Φ_{quench} using our model for a group of experimental systems described in the literature and compared the predicted Φ_{quench} with the measured Φ_{quench} . Measurement of Φ_{quench} by itself is not common, and accurate measurements can be challenging because of rapid back electron transfer, low cage escape yields, or other unproductive pathways.^{13–15} Mindful of this, we carefully selected a set of trial reactions where Φ_{quench} was known independently of other unproductive pathways. Figure 2 shows the comparison between predicted

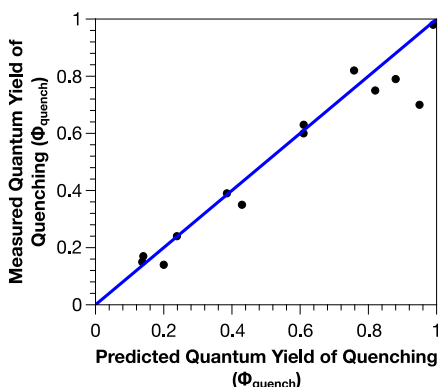


Figure 2. Predicted quantum yields of quenching (Φ_{quench}) compared to experimentally measured quantum yields of quenching (Φ_{quench}). Solid blue line shows one-to-one correlation. Details of the measured quantum yields are provided in the Supporting Information.

and measured Φ_{quench} and demonstrates an excellent correlation, suggesting that our kinetic modeling method produces values in good agreement with the experiment.

We propose that eq 3 can be a useful tool in evaluating the reaction design. Using a series of photoredox reactions that rely on acridinium-based photocatalysts (PCs), we compared the quencher concentrations used in experimental reports to the concentration of quencher predicted by eq 3. Acridinium-based PCs are commonly used in photoredox reactions and typically exhibit short lifetimes on the order of 10 ns.¹⁶ Figure 3 shows that the majority of experimental reports we evaluated used less quencher than what eq 3 predicts, which is needed for efficient quenching. It is also notable that the deviation becomes more pronounced at smaller values of k_q . This is largely a function of most reports using a quencher concentration on the order of 0.1–0.2 M. While this concentration range is appropriate for larger values of k_q ($10^9 \text{ M}^{-1} \text{ s}^{-1}$ or greater), it is too low for smaller values of

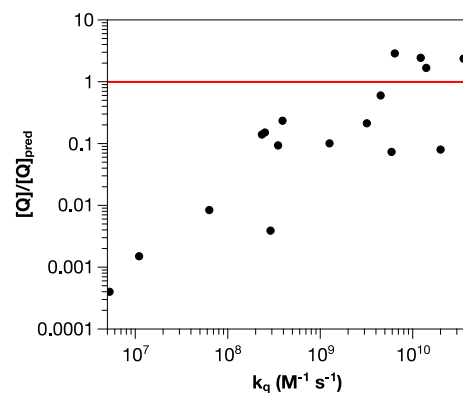


Figure 3. Ratio of experimental quencher concentration to predicted quencher concentration from eq 3 as a function of quenching rate constant, k_q , for 18 examples of photoredox reactions using acridinium-based PCs. Solid red line indicates a ratio of 1:1 for the experimental-to-predicted quencher concentration. Details for each experimental study are provided in the Supporting Information.

k_q . It is important to note that using a quencher concentration that is too low will impact the quantum yield of the reaction, but not necessarily the overall product yield, as most of the reactions surveyed in Figure 3 achieve product yields of 70% or higher. However, the majority of the reactions ran for more than 24 h and utilized extremely bright light sources. This suggests that the quantum yields of these reactions are indeed low and may prove to be an issue when considering the energy intensity of these photoredox reactions.¹⁷ More generally, this suggests that photoredox reactions that rely on PCs with short lifetimes, that is, those on the nanosecond timescale, will struggle to achieve high quantum yields unless paired with substrates that exhibit a large k_q .

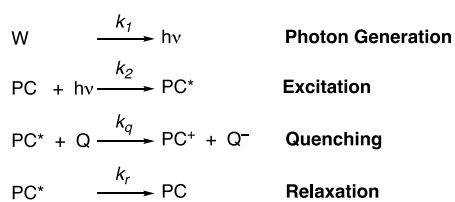
CONCLUSIONS

In analogy with multistep synthetic reactions, the overall reaction quantum yield for a photochemical reaction is the product of yield for each individual step. Ensuring a high Φ_{quench} offers the best chance of achieving a high quantum yield for the overall reaction and is the step that can be most easily impacted via experimental design. Using kinetic modeling, we have shown that the quencher concentration needed for efficient excited state quenching (90% or greater) is simply predicted by the Stern–Volmer equation and relies only on τ and k_q , two parameters that are readily accessible. Considering the design of photoredox reactions from a quantum yield perspective, eq 3 predicts that optimal PC lifetimes in the microsecond to tens of microsecond range would be needed to use quencher concentrations on the order of hundreds of millimolar.

METHOD

Reactions were simulated using Kinetiscope (<https://hinsberg.net/kinetiscope/>). Scheme 2 shows a typical reaction setup. A simple reaction scheme was used that involved the excitation of a PC and then a competition between relaxation and quenching. The excitation was handled in two steps following our previous work.⁷ In the first step, photon generation, photons were generated via a zeroth-order reaction at a rate of 1.63×10^{-5} photons/s. This simulates 10 mW illumination at 415 nm. In the next step, excitation, the photons were captured by the PC to generate the excited photocatalyst (PC*) at a rate

Scheme 2. Steps Used in Kinetic Modeling of Quantum Yields



of $1 \times 10^{14} \text{ M}^{-1} \text{ s}^{-1}$. An arbitrarily large rate constant was selected to ensure that every time a photon interacted with a PC, excitation occurred. This also ensured efficient capture of all photons, with the simulation modeling continuous, uniform excitation across the reaction volume. While in a real system absorption of photons would be governed by the Beer–Lambert–Bouguer law, we are not specifying a specific PC and, by extension, molar extinction coefficient. Even in a real system with high PC concentrations and a large molar extinction coefficient at the excitation wavelength, the instantaneous concentration of excited PC generated by constant illumination would be 13 orders of magnitude smaller than the quencher concentrations used in this study.

After excitation, the excited PC could then relax back to the ground state ($PC^* \rightarrow PC$), relaxation, or be quenched by a quencher in the pathway labeled “quenching”. Though the quenching step was written as an oxidative quenching reaction, the results would be identical for a reductive quenching or energy transfer. In order to simplify the analysis, no back electron transfer between PC^+ and Q^- was allowed to occur nor was PC^+ regenerated. In this study, we investigated the quantum yield of quenching, Φ_{quench} , which is simply defined as the number of PCs that undergo quenching divided by the number of excited PCs. This parameter is unaffected by other reaction pathways (e.g., back electron transfer), and so to simplify the model, no other pathways were included. The simulation length was 1 s, which decreased the simulation running time and ensured that only a small concentration of PC was converted into PC^+ by the end of the simulation. Φ_{quench} results were unchanged when running the simulation for longer timescales or when adding in a PC regeneration step.

For steady-state illumination simulation, a PC concentration of 100 μM was used, while for simulations involving a fixed initial concentration of PC^* , a concentration of 1 μM was used. In Kinetiscope, individual particles are used to track ensembles of molecules. Variation of the number of moles represented by a given particle showed no effect on Φ_{quench} for steady-state illumination but some deviation in Φ_{quench} for a fixed concentration of PC^* (Figure S1). As a result, the total number of particles was adjusted so that there was 10^{-13} mol/particle. For constant illumination, the simulation ran for 1 s, and the concentration of Q varied until a Φ_{quench} value of 0.900 ± 0.001 was achieved at the end of the reaction. For a fixed starting concentration of PC^* , the concentration of Q was varied until Φ_{quench} at 100 ns equaled 0.900 ± 0.001 .

Simulation of published reactions followed an identical approach as above with minor modifications. The concentration of Q used in the simulation was the same as that used in the published report and was not varied. Where possible, the concentration of PC used matched that in the published report. If the concentration of PC was not reported, a value of 100 μM was utilized. The concentration of PC was found to

have no impact on the quantum yield of the reaction unless the concentration of PC was less than 20 μM .

■ ASSOCIATED CONTENT

Supporting Information

The Supporting Information is available free of charge at <https://pubs.acs.org/doi/10.1021/acsomega.2c02638>.

Details of kinetic modeling; impact of illumination time and intensity on quantum yield; predicted quencher concentrations for starting with the fixed concentration of excited PC; comparison of quencher concentrations predicted by eq 3 with those derived from kinetic modeling; and details of experimental studies included in Figures 2 and 3 (PDF)

■ AUTHOR INFORMATION

Corresponding Author

John R. Swierk – Department of Chemistry, State University of New York at Binghamton, Vestal, New York 13850, United States; orcid.org/0000-0001-5811-7285; Email: jswierk@binghamton.edu

Author

Xena L. Soto – Department of Chemistry, State University of New York at Binghamton, Vestal, New York 13850, United States; Department of Chemistry, Lehman College/City University of New York, Bronx, New York 10468, United States

Complete contact information is available at:

<https://pubs.acs.org/doi/10.1021/acsomega.2c02638>

Notes

The authors declare no competing financial interest.

■ ACKNOWLEDGMENTS

This work was supported by the National Science Foundation (NSF CHE-2047492). X.L.S. thanks the State University of New York Louis Stokes Alliance for Minority Participation (NSF 1619619) for a summer research fellowship. Finally, the authors wish to acknowledge ChemRxiv for publishing an earlier version of this manuscript as a preprint.¹⁸

■ REFERENCES

- (1) Arias-Rotonda, D. M.; McCusker, J. K. The Photophysics of Photoredox Catalysis: A Roadmap for Catalyst Design. *Chem. Soc. Rev.* **2016**, *45*, 5803–5820.
- (2) Pitre, S. P.; McTiernan, C. D.; Scaiano, J. C. Understanding the Kinetics and Spectroscopy of Photoredox Catalysis and Transition-Metal-Free Alternatives. *Acc. Chem. Res.* **2016**, *49*, 1320–1330.
- (3) Prier, C. K.; Rankic, D. A.; MacMillan, D. W. C. Visible Light Photoredox Catalysis with Transition Metal Complexes: Applications in Organic Synthesis. *Chem. Rev.* **2013**, *113*, 5322–5363.
- (4) Narayanam, J. M. R.; Stephenson, C. R. J. Visible Light Photoredox Catalysis: Applications in Organic Synthesis. *Chem. Soc. Rev.* **2011**, *40*, 102–113.
- (5) Romero, N. A.; Nicewicz, D. A. Organic Photoredox Catalysis. *Chem. Rev.* **2016**, *116*, 10075–10166.
- (6) Wu, Y.; Kim, D.; Teets, T. S.; Photophysical Properties and Redox Potentials of Photosensitizers for Organic Photoredox Transformations *Synlett* **2022**; Vol. 33, 1154–1179.
- (7) Stevenson, B. G.; Spielvogel, E. H.; Loiaconi, E. A.; Wambua, V. M.; Nakhmiiyayev, R. V.; Swierk, J. R. Mechanistic Investigations of an α -Aminoarylation Photoredox Reaction. *J. Am. Chem. Soc.* **2021**, *143*, 8878–8885.

(8) Spielvogel, E. H.; Stevenson, B. G.; Stringer, M. J.; Hu, Y.; Fredin, L. A.; Swierk, J. R. Insights into the Mechanism of An Allylic Arylation Reaction via Photoredox Coupled Hydrogen Atom Transfer. *J. Org. Chem.* **2022**, *87*, 223–230.

(9) Hinsberg, W. D.; Houle, F. A. Kinetiscope. <http://www.hinsberg.net/kinetiscope> (accessed May 12, 2019).

(10) Liu, M. J.; Wiegel, A. A.; Wilson, K. R.; Houle, F. A. Aerosol Fragmentation Driven by Coupling of Acid-Base and Free-Radical Chemistry in the Heterogeneous Oxidation of Aqueous Citric Acid by OH Radicals. *J. Phys. Chem. A* **2017**, *121*, 5856–5870.

(11) Bolshchikov, B. D.; Tsvetkov, V. B.; Alikhanova, O. L.; Serbin, A. V. How to Fight Kinetics in Complex Radical Polymerization Processes: Theoretical Case Study of Poly(divinyl ether-alt-maleic anhydride). *Macromol. Chem. Phys.* **2019**, *220*, 1900389.

(12) Bonaldo, F.; Mattivi, F.; Catorci, D.; Arapitsas, P.; Guella, G. D Exchange Processes in Flavonoids: Kinetics and Mechanistic Investigations. *Molecules* **2021**, *26*, 3544.

(13) Olmsted, J.; Meyer, T. J. Factors Affecting Cage Escape Yields Following Electron-Transfer Quenching. *J. Phys. Chem.* **1987**, *91*, 1649–1655.

(14) Sun, H.; Hoffman, M. Z. Reductive Quenching of the Excited State of Ruthenium(II) Complexes Containing 2,2'-Bipyridine, 2,2'-Bipyrazine, and 2,2'-Bipyrimidine. *J. Phys. Chem.* **1994**, *98*, 11719–11726.

(15) Aydogan, A.; Bangle, R. E.; Cadranel, A.; Turlington, M. D.; Conroy, D. T.; Cauët, E.; Singleton, M. L.; Meyer, G. J.; Sampaio, R. N.; Elias, B.; Troian-Gautier, L. Accessing Photoredox Transformations with an Iron(III) Photosensitizer and Green Light. *J. Am. Chem. Soc.* **2021**, *143*, 15661–15673.

(16) Joshi-Pangu, A.; Lévesque, F.; Roth, H. G.; Oliver, S. F.; Campeau, L.-C.; Nicewicz, D.; DiRocco, D. A. Acridinium-Based Photocatalysts: A Sustainable Option in Photoredox Catalysis. *J. Org. Chem.* **2016**, *81*, 7244–7249.

(17) Ruccolo, S.; Qin, Y.; Schnedermann, C.; Nocera, D. G. General Strategy for Improving the Quantum Efficiency of Photoredox Hydroamidation Catalysis. *J. Am. Chem. Soc.* **2018**, *140*, 14926–14937.

(18) Soto, X.; Swierk, J. Using Lifetime and Quenching Rate Constant to Determine Quencher Concentration. *ChemRxiv*, *26*, **2022**. ver. 1. DOI: [10.26434/chemrxiv-2022-q6klm](https://doi.org/10.26434/chemrxiv-2022-q6klm).